Running title: ASHR3 SET-domain protein controls root cell cycles

Corresponding author: Reidunn B. Aalen, Department of Biosciences, University of Oslo, P.O. Box 1066 Blindern, N-0316 Oslo, Norway.

E-mail: reidunn.aalen@ibv.uio.no. Phone: +47 22854437

Special Issue: **Roots**

Research area: **Genes, Development and Evolution**

Secondary area: **Cell biology**

The ASHR3 SET-domain Protein Controls Cell Division Competence of the Meristem and Quiescent Centre of the *Arabidopsis thaliana* Primary Root

Robert Kumpf[2,3], Tage Thorstensen[2,3], Mohummad Aminur Rahman[3], Jefri Heyman[3], H. Zeynep Nenseth, Tim Lammens[3], Ullrich Herrmann, Ranjan Swarup, Silje Veie Veiseth, Gitika Emberland, Malcolm J. Bennett, Lieven De Veylder and Reidunn B. Aalen*

Department of Biosciences, University of Oslo, N-0316 Oslo, Norway (R.K., T.T., M.A.R., H.Z.N., U.H., S.V.V., G.E., R.B.A.); Department of Plant Systems Biology, VIB, and Department of Plant Biotechnology and Bioinformatics, Ghent University, B-9052 Ghent, Belgium (J.H., T.L., L.D.V.); Centre for Plant Integrative Biology, University of Nottingham, UK (R.S., M.J.B.)

The ASHR3 histone lysine methyltransferase gene is expressed in the root stem cell niche and contributes to co-ordinated divisions of daughter, grand-daughter and great-granddaughter cells originating from the same stem cell.

[1] This work was supported by the Research Council of Norway (grant 146652/431), and the Interuniversity Attraction Poles Programme (IUAP P7/29 "MARS"), initiated by the Belgian Science Policy Office.

[2] These authors contributed equally to this article.

[3] Present addresses: Department of Plant Systems Biology, VIB, B-9052 Ghent University, Belgium (R.K.); Bioforsk, N-1432 Ås, Norway (T.T.); Oncomatrix Research Laboratory, Department of Biomedicine, University of Bergen, N-5009 Bergen, Norway (M.A.R.); Centrum voor Medische Genetica, Ghent University, B-9000 Ghent, Belgium (T.L.)

[*] Address correspondence to reidunn.aalen@imbv.uio.no.

Keywords: histone modification, meristem length, Chromatin Immuno Precipitation (ChIP), Quiescent Centre, H3K36me1, H3K36me2

The stem cell niche (SCN) of the *Arabidopsis thaliana* primary root apical meristem is composed of the quiescent (or organising) centre (QC) surrounded by stem (initial) cells for the different tissues. Initial cells generate a population of transit amplifying cells that undergo a limited number of cell divisions before elongating and differentiating. It is unclear whether these divisions occur stochastically or in an orderly manner. Using the thymidine analogue EdU to monitor DNA replication of cells of Arabidopsis root meristems we identified a pattern of two, four and eight neighbouring cells with synchronized replication along the cortical, epidermal and endodermal cell files, suggested to be daughters, granddaughters and great-granddaughters of the direct progeny of each stem cell. Markers of mitosis and cytokinesis were not present in the region closest to the transition zone where the cells start to elongate, suggesting that great-granddaughter cells switch synchronously from the mitotic cell cycle to endoreduplication. Mutations in the SCN-expressed *ASH1 RELATED3* (*ASHR3*) gene, encoding a SET-domain protein conferring histone H3 lysine 36 methylation, disrupted this pattern of co-ordinated DNA replication and cell division, and increased the cell division rate in the QC. E2Fa/E2Fb transcription factors controlling the G1-to-S phase transition regulate *ASHR3* expression and bind to the *ASHR3* promoter, substantiating a role for ASHR3 in cell division control. Reduced length of the root apical meristem and primary root of the mutant *ashr3-1* indicate that synchronization of replication and cell divisions is required for normal root growth and development.

INTRODUCTION

Root growth depends on the continuous generation of new cells in the root tip. The root apical meristem (RAM) is composed of three main zones, determined by their cellular features, namely the stem cell niche (SCN); the proximal meristematic zone (MZ) where cell division occurs, and the basal meristem, a transition zone (TZ) where cells start to elongate (Bennett and Scheres, 2010; Perilli and Sabatini, 2010; Perilli et al., 2012). The SCN comprises the quiescent centre (QC) (Fig. 1A), consisting of cells mitotically less active than the surrounding stem cells (initials). From the initials daughter, granddaughter and great-granddaughter cells are continuously produced in cell files of the MZ, ensuring a steady generation of new cells which will elongate and differentiate and thereby contribute to root growth and development (Jiang and Feldman, 2005; Moubayidin et al., 2010; Perilli and Sabatini, 2010).

Exit from the MZ has been though to coincide with a switch from the mitotic cycle to an endoreduplication cycle where the DNA is duplicated but no cytokinesis occurs (De Veylder et al., 2011). Recent evidence suggests that endoreduplication precedes rapid cell elongation (Hayashi et al., 2013). Whilst proteins that control the switch to the endocycle have been described (De Veylder et al., 2011; Heyman and De Veylder, 2012), molecular components that control the maintenance of cell division in the MZ have not been identified to date. Like animals, plants control the entry into the S-phase of the cell cycle by the E2F-Retinoblastoma (Rb) pathway (Weinberg and 1995; Berckmans and De Veylder, 2009). Rb in animals and RB-RELATED1 (RBR1) in Arabidopsis are repressors of E2F transcription factors, and *RBR1* over-expression results in rapid loss of stem cell identity of root initials (Wildwater et al., 2005). Arabidopsis encodes three E2Fs (E2Fa, E2Fb, and E2Fc) that need to associate with one out of two dimerization partners (DPa and DPb) to be active (Berckmans and De Veylder, 2009). E2Fa in association with DPa induces cell proliferation and increases ploidy levels (De Veylder et al., 2002). Likewise, E2Fb encodes an activator of cell

proliferation, whereas E2Fc rather operates as repressor (Magyar et al., 2005; del Pozo et al., 2006). E2F target genes have a cell-cycle-modulated G1- or S-phase expression profile. Genes likely to be directly regulated by E2Fa-DPa in Arabidopsis have specific binding sites with a *WTTSSCSS* (where W = A or T, and S = G or C) *cis*-acting consensus element in their promoter region (Vandepoele et al., 2005; Naouar et al., 2009). More than 300 such genes have been identified, including a number homologous to mammalian E2F target genes controlling replication and chromatin structure (Vandepoele et al., 2005; Naouar et al., 2009).

Deposition of appropriate epigenetic marks is necessary for expression of cell cycle-related genes, for labelling of replication origins, and during the S-phase for maintenance of epigenetic signatures on new DNA double helices, e.g. signatures that will regulate gene expression and establish eu- and heterochromatin (Costas et al., 2011; Dorn and Cook, 2011). SET-domain proteins represent important chromatin-modifiers responsible for mono-, di- or trimethylation of various lysine residues on N-terminal histone tails (Kouzarides, 2007; Liu et al., 2010; Thorstensen et al., 2011). In search for SET-domain proteins operating during the cell cycle, we identified the SCN-expressed Arabidopsis gene *ASH1 RELATED3 (ASHR3)* (Baumbusch et al., 2001). Here we present genetic and molecular data indicating that *ASHR3* is a direct target for E2F transcription factors. *ASHR3* appears important for maintenance of meristematic cell divisions based on comparison of cell length and cell number in wild type (Wt) and *ashr3-1* MZs cell files: By monitoring of DNA replication using the thymidine analogue EdU. a co-ordinated pattern of replication along the entire epidermal, cortical and endodermal MZ cell files was revealed. Mitosis and cytokinesis markers displayed a similar pattern, but were only present in 2/3 of the MZ, closest to the QC. The co-ordinated patterns of replication and cell divisions were distorted in the *ashr3-1* mutant. Furthermore, in the *ashr3-1* QC we observed a higher number of cells and more cells undergoing DNA replication, suggesting that the quiescence of these cells is abrogated. Chromatin Immuno

Precipitation (ChIP) indicated that ASHR3 acts as a histone H3 lysine 36 (H3K36) monomethyltransferase to facilitate co-ordinated replication patterns in the root MZ.

RESULTS

The *ashr3* Mutation Affects Root Apical Meristem Development and Organisation

The Arabidopsis primary root displays a well-ordered symmetric pattern of cells in the RAM and the SCN (Fig. 1A). *ASHR3* is one of the few genes encoding SET domain proteins reported to be expressed in the QC and surrounding cells (Table I). The *ASHR3* promoter-reporter construct *pASHR3:GUS* (Thorstensen et al., 2008) was expressed in the SCN region (Fig. 1A), thus confirming the microarray data (Nawy et al., 2005). The T-DNA insertion mutant *ashr3-1,* with > 90% reduction in the *ASHR3* transcript level (Fig. S1A-B), was inspected for aberrant root phenotypes. A growth assay showed that *ashr3-1* roots were significantly shorter than Wt roots 10 days after germination (DAG) when, under our growth conditions the root meristem is fully developed (Fig. 1B). Introduction of a Wt copy of the *ASHR3* gene in the mutant restored the root length. Anatomical measurements of confocal images of propidium iodide (PI) stained roots, disclosed significantly shorter MZ in the mutant compared to Wt from 10 DAG, while at 6 DAG, the size of the *ashr3-1* MZ was similar to wild type (Fig. S1C). In the Wt, cells double in length and then divide (Ubeda-Tomas et al., 2009). Inspection of images of 6 DAG PI stained roots suggested that mutant cells grew larger than Wt cells before undergoing cell divisions (Fig. 1C-D and Fig. S1D). In both Wt and mutant MZs the distal cells near the QC were smaller than the proximal cells, however, on the average, *ashr3-1* meristematic cortical cell were longer than the Wt cells (10.6 ± 0.9 and 8.7 ± 1.1 μm, respectively, Student's *t*-test $P = 6.8\ 10^{-3}$, based on 7 and 10 cell files of mutant and Wt roots; Fig. 1C, and Fig. S1E). Introduction of the Wt *ASHR3* gene resulted in a cellular pattern and shortened MZ cells similar to Wt (P = 0.064) (Fig. S1E-F).

The larger mutant cell size, which was also observed for differentiated mature cortex cells (Fig. S1G) may explain the minor difference in MZ length and total length of young *ashr3-1* roots.

Upon closer inspection of the SCN we observed aberrant cellular organisation and division planes in the *ashr3-1* columella root cap (CRC) and the QC (Fig. 1E), a phenotype that also was rescued by complementation with the Wt *ASHR3* gene (Fig. S1H).

The Pattern of Co-ordinated Replication is Perturbed in the *ashr3-1* Mutant

To substantiate an aberrant cell division phenotype, DNA replication in 10 days old roots was monitored using an one-hour pulse treatment with EdU, a nucleoside analogue of thymidine that is incorporated in DNA undergoing replication. The number and positions of replicating nuclei along the cortex, epidermis and endodermis cell files were registered. Near the QC about 10% of the cortical cells were replicating in the Wt, and after cell 16, 35-40 % (Fig. 2A). In the *ashr3-1* mutant the replication activity was similar in the apical part of the meristem (cells 1-16), but lower than the Wt in the proximal part (cells 17-40) (Fig. 2A).

In the Wt we observed a non-random distribution of neighbouring replicating cells along the cortical, epidermal and endodermal cell files (Fig. 2B and Supplemental Fig. S2). The frequency and distribution of neighbouring co-replicating cells in the cortex (inspected in 16 cell files, delimited to 40 cells) clearly diverged from a stochastic pattern. There was 1) an overrepresentation of two, four and eight neighbouring replicating cells and an absence or strong underrepresentation of triplets, quintets, sextets and septets (Fig. 2C and Table II); 2) a spatial distribution with a region exclusively of singlets in the first few cells nearest the QC with a subsequent rapid decline of singlets; 3) an abundance of duplets in cell positions 5-8; 4) a concentration of quartets in cells 17-20; and 5) a rise in octets from cell 24 (Fig. 2D). Similar co-replication frequencies and patterns of distribution were seen for the endodermal and epidermal cell files (Fig. S2A-E and Table II), however, in the epidermis both quartets

and octets were abundant from cell 28 (Fig. S2E). Co-ordinated replication of adjacent cells belonging to different cell layers was not observed.

In the *ashr3-1* mutant the relative abundance of the categories of co-replicating cells in the cortex, epidermis and endodermis deviated significantly from the Wt (Fig. 2C, Fig. S2B-C and Table II), as duplets in particular were overrepresented whereas octets were not found. Additionally, the frequency of quartets was reduced and/or the quartets appeared more distantly from the QC in *ashr3-1* than in the Wt (Fig. 2D-E and Fig. S2D-G).

Interestingly, very few replicating cells were found present in the stele of the *ashr3-1* mutant line (Fig. 2B and Fig. S2A), while at the same time the number of cells in the meta- and anaphase were significantly higher than in the Wt (Fig. 2B, Fig. S2A, and Table II). Together, this suggested that loss of *ASHR3* interferes with cell cycle progression.

Cell Divisions are Less Co-ordinated in *ashr3-1* Roots

To detect putative differences in mitotic activity, we monitored cell cycle progression by using a CYCB1;1-GUS reporter (Colón-Carmona et al., 1999), and cytokinesis by immune localisation of the KNOLLE protein, a syntaxin involved in formation of the cell plate between separating sister cells (Lauber et al., 1997). Both approaches substantiated the role of *ASHR3* in co-ordination of the cell cycle in neighbouring cells: in 6 DAG roots the Wt CYCB1;1-GUS was predominantly expressed in files of neighbouring cells, while in *ashr3-1* expression was characteristically confined to several single cells (Fig. 2F-G and Fig. S3A). KNOLLE was identified in neighbouring cells undergoing cytokinesis in the Wt, while this was observed infrequently in of images of *in situ* immune localization in *ashr3-1* 3 DAG root meristems (Fig. 2H and Fig. S3B). Maximal projection of the confocal images suggested in addition that more cells underwent cytokinesis in the Wt versus *ashr3-1* (Fig. 2I).

In contrast to DNA replication detected using EdU (Fig. 2A) neither CYCB1;1-GUS nor KNOLLE were localized in the entire MZ (Fig. 2G-I). CYCB1;1-GUS protein was found in a region stretching from the QC to encompass 24.6±3.3 Wt and 26.3±3.6 *ashr3-1* cortical cells (a non-significant difference, Student's *t*-test P = 0.22, N = 15). Similarly, in 3 DAG roots KNOLLE localization was rarely found in the proximal third part of the MZ (Fig. 2H-I and Fig. S3B).

A Functional *ASHR3* Gene is Needed to Maintain QC Quiescence

Due to aberrant cellular patterning in *ashr3-1* SCN (Fig. 1A), DNA replication in this region was studied in more detail. In the Wt two-to-three QC cells can be observed in a single focus plane using CLSM and Nomarski optics with DIC (Fig. 3A). In contrast, in nine out of ten cases the *ashr3-1* QCs encompassed more cells, even up to twelve cells expressing QC-specific markers like *pWOX5:GUS* and *QC46:GUS* (Fig. 3B-C). These cells were found near the stem cells of the endodermis/cortex and epidermis/lateral root cap (LRC) (Fig. 3B). Consistent with this observation, a one-hour EdU pulse failed to capture replication of Wt QC cells, but revealed replication in QC cells close to the endodermis/cortex and epidermis/LCR initials in eight out of ten *ashr3-1* roots (Fig. 3D-E). Starch granules indicative of CRC differentiation were absent in the CRC stem cell layer D1 closest to the QC, just like in Wt roots (Fig. 3F-G), suggesting that the rate of differentiation of the CRC cells was not affected by the increase in QC cell divisions.

***ASHR3* is a Target of E2Fa/E2Fb and Expressed During S-Phase**

To substantiate a link to the cell cycle, we investigated whether expression of *ASHR3* was cell cycle phase-dependent using synchronized Arabidopsis suspension culture cells. The majority

of cells duplicate their DNA content from 2C to 4C within the first four hours of the experiment. During this period the *ASHR3* transcript level peaked (Fig. 4A), showing that *ASHR3* is a S-phase regulated gene, confirming previous microarray data (Menges et al., 2003). The G1-to-S cell cycle transition is controlled by the E2Fa/E2Fb-DPa transcription factor complex. Consistent with detection of *E2Fa* mRNA in the root meristem including the SCN (De Veylder et al., 2002), an E2Fa-GFP fusion protein, generated from a construct controlled by E2Fa's own promoter, was found present in QC and initial cells, as well as the MZ cells (Fig. S4) (Magyar et al., 2012). We therefore investigated whether *ASHR3* was regulated by these transcription factors. In agreement with microarray data (Genevestigator, https://www.genevestigator.com/gv/plant.jsp; (Vandepoele et al., 2005)) *ASHR3* was strongly induced in transgenic lines overexpressing *E2Fa-DPa* (*E2Fa-DPa*^{OE}), being about 30-fold more abundant than in Wt seedlings (Fig. 4B). The *ASHR3* expression level was reduced in an *e2fa-2* but not an *e2fb-1* mutant background, however, a strong reduction in transcripts levels was observed in an *e2fa-2 e2fb-1* double mutant, suggesting that E2Fa and E2Fb redundantly control *ASHR3* expression similarly to their control of *ULTRAVIOLET-B-INSENSITIVE4* (*UVI4*) (Fig. 4B) (Heyman et al., 2011).

The *ASHR3* promoter holds two potential consensus E2F-DP binding sites (-186 ATTGCCCC (reverse) and -123 TCTCCCGC) (Vandepoele et al., 2005; Naouar et al., 2009). Binding of E2Fa-DPa to the latter sequence was demonstrated by electrophoretic mobility shift assay (EMSA) using a mutant version (TCTCCATC) as a negative control (Fig. 4C). Furthermore, Chromatin Immune Precipitation (ChIP) using anti-E2Fa antibodies resulted in an enrichment of a *ASHR3* promoter fragment encompassing the putative E2F binding sites, at a level previously shown for the *UVI4* promoter (Heyman et al., 2011), compared with the actin-negative control (Fig. 4D). These data show that E2F transcription factors can bind to the *ASHR3* promoter and regulate its expression.

ASHR3 Confers Histone H3 Lysine 36 Methylation

ASHR3 is a member of the ASH1/Set2 subgroup of histone lysine methyltransferases (HKMTases) which are associated with transfer of methyl groups to histone H3 lysine 36 (H3K36), and in Arabidopsis this subgroup encompasses four *ASH1 HOMOLOG* (*ASHH1-4*) genes and two additional *ASH1 RELATED* (*ASHR1-2*) genes (Baumbusch et al., 2001; Thorstensen et al., 2011). To identify a link between mutant phenotypes and ASHR3's expected function as an HKMTase, we performed ChIP experiments on one-week-old seedlings using antibodies against H3K36 monomethyl (H3K36me1) and H3K36me2. Irrespective of gene expression levels in the Wt control and *ashr3-1* mutant background (Fig. S5A-B), all the genes tested, including housekeeping genes (*ACTIN2* and *TUBULIN8*); genes encoding regulators of transcription (*JAZ1* and *WRKY40*); transcriptionally silent, late replicating transposable elements (TEs) (*Ta3*, *TSI* and *CACTA*); and genes reported to contain active replication origins in Arabidopsis cell cultures (*ALLENE OXIDE SYNTHASE* (*AOS*) and *LIPOXYGENASE3* (*LOX3*) (Costas et al., 2011)); turned out to have reduced H3K36me1 levels (Fig. 5A). The H3K36me2 levels differed in general less between Wt and mutant, with the exception for *WRKY40* and *LOX3*. Prominent *ASHR3* expression has not been observed aboveground in seedlings (Thorstensen et al., 2008), and the lower H3K36me level in *ashr3-1* seedlings may therefore predominantly be ascribed to reduced expression level in the root cells where *ASHR3* normally is expressed. This includes the SCN, and additionally, cells surrounding the base of emerged lateral roots (Thorstensen et al., 2008). ChIP on chromatin from inflorescences, where *ASHR3* is strongly expressed in Wt developing anthers (Thorstensen et al., 2008), also showed reduced H3K36me1 levels and to some extent H3K36me2 levels for the mutant (Fig. S5), substantiating the link between *ASHR3* and H3K36 HKMTase activity.

DISCUSSION

ASHR3 is the First SET-Domain Protein Associated with H3K36 Mono-Methylation

The consistent reduction of H3K36me1 levels on genes and TEs in the *ashr3-1* mutant advocates ASHR3 as the first SET-domain protein identified to date with histone H3K36 mono-methyltransferase activity. The additional reduction in H3K36me2, an euchromatic mark genome-wide associated with transcribed genes (Oh et al., 2008), indicates that ASHR3 also may have dimethyltransferase activity, and/or provides H3K36me1 as a substrate for a dimethyltransferase. Hence, ASHR3 may mediate both transcription-independent H3K36me1 and transcription-associated H3K36me2. The residual H3K36me1 present at all loci tested suggests that there are more Arabidopsis HKMTases with H3K36me1 product specificity. Likely candidates are the ASHH and ASHR proteins for which the specificity has not been determined yet (Baumbusch et al., 2001; Thorstensen et al., 2011). As the *ashr3-1* single mutant displays a phenotype, these HKMTases are at most partially redundant with ASHR3, and may act in different cellular and epigenetic contexts.

Several lines of evidence argue that *ASHR3* is a direct target of E2Fa/E2Fb transcription factors that control S-phase dependent gene expression. Reduced *ashr3-1* transcript levels in the *ef2a-2 ef2b-1* double mutant indicate that *ASHR3* might be redundantly regulated by E2Fa/E2Fb. *In vitro* EMSA confirmed binding of the promoter sequence postulated to have an E2F binding site. This was substantiated by ChIP, and is also supported by a recent study where tandem chromatin affinity purification (TChAP) was used to identify targets of E2Fa (Verkest et al., 2014). This, together with cell-cycle regulated *ASHR3* expression in cell culture, the *ashr3-1* mutant root phenotype affecting replication and cell division, and importantly, the overlapping expression patterns of E2Fa and *ASHR3* in the SCN makes it conceivable that *ASHR3* is part of the E2F-dependent regulation of root apical meristem function.

Of the near to 40 genes encoding SET-domain proteins in Arabidopsis (Baumbusch et al., 2001; Thorstensen et al., 2011), cell cycle regulation has previously been documented only for *ATXR5* and *ATXR6*, encoding H3K27me1 HKMTases associated with replication of heterochromatin (Raynaud et al., 2006; Jacob et al., 2009; Jacob et al., 2010). As ASHR3 has predominantly eukaryotic localization and different HKMTase specificity, it is likely to have a function that differs from the *ATXR* genes. In fission yeast H3K36 methylation has been implicated in replication fork stabilization and checkpoint activation (Kim et al., 2008). In budding yeast replication factors have highest preference for non-transcribed euchromatin with high H3K36me1 and the abundance of H3K36me1 increases at origins of replication throughout the S phase (Pryde et al., 2009). Arabidopsis origins identified in cell cultures have been reported preferably to reside in the 5' half of genes, be enriched in histone H2A.Z, H3K4me2/me3 and H4K5ac, and depleted in H3K4me1 and H3K9me2 (Costas et al., 2011). We have identified transcription-independent ASHR3-dependent H3K36me1 both at such suggested origins of replication in the *AOS* and *LOX3* genes, and on other genes presumably further away from origins (Costas et al., 2011), but to date it is not known whether these origins are used in tissues of intact plants.

Daughter, Grand-Daughter and Great-Granddaughter Cells in Meristematic Cell Files Exhibit ASHR3-Dependent Synchronized Replication

To monitor DNA replication in the MZ we have used a one-hour pulse with EdU, as a short EdU pulse facilitates the identification of cells replicating at the same time (Hayashi et al., 2013). Our EdU experiment revealed an ASHR3-dependent pattern where neighbouring co-replicating cells preferably come in duplets, quartets and octets, with a non-random distribution along the MZ. To explain this pattern we have developed a simple model suggesting that the progeny of each direct descendant (singlet) of a dividing epidermal,

cortical or endodermal stem cell will go through three-to-four consecutive synchronized rounds of cell division to give rise to duplets, quartets and octets of co-replicating neighbouring daughter, granddaughter and great-granddaughter cells along the MZ (Fig. 6A). Beside the pattern of distribution, the most compelling support for this model is the lack or underrepresentation of co-replicating triplets, quintets, sextets and septets. The overrepresentation of quartets in the proximal part of the epidermal cell files, where the model predicts octets, can most likely be ascribed to differences between root-hair cells (trichoblasts), reported to have the same length and cell division characteristics as cortical cells, and the longer non-hair cells (atrichoblasts) (Beemster and Baskin, 1998). With a given length of the MZ the fewer but longer atrichoblasts cells may reach the TZ and exit from the MZ with one round of replication less than the atrichoblasts, cortical and endodermal cells.

EdU incorporation showed that a normal frequency of DNA replication was dependent of ASHR3 both in the quartet and octet region, and confirmed that DNA replication takes place from the QC to the TZ where cells start to elongate, i.e. in the entire region defined as MZ (Ubeda-Tomas et al., 2009). Synchronized mitosis and cytokinesis in neighbouring cells seem also to be ASHR3-dependent, but in contrast to DNA replication, both the mitosis CYCB1;1-GUS and the cytokinesis KNOLLE markers (Ubeda-Tomas et al., 2009) demonstrated that cell divisions basically are confined to the first two thirds of the defined MZ cells. The region with cell divisions (stopping at 24.6±3.3 Wt cortical cells) corresponds well to our simple working model with on average 4 initials dividing into 8 doublet daughter cells, giving rise to 16 quartet granddaughter cells which will replicate and divide, that is 28 cells where cell division will occur (Fig. 6A-C). The last round of replication, seen in co-replicating octets of presumed great-granddaughters of dividing initials, must therefore be replication without cytokinesis, the process known as endoreduplication. This is also

suggested from the large cells with big EdU labelled nuclei near the transition zone seen in our images (Fig. 6D) and described recently as 4C cells by (Hayashi et al., 2013).

A key feature of our working model is a need for a mechanism that identifies cells of the same generation so that they can be induced to behave co-ordinated. An epigenetic mark would be ideal for such a purpose, since without renewal during replication the level of a histone PTM will be halved for each cell division (Hake and Allis, 2006). Incorporation of a PTM in chromatin of the QC and stem cells, followed by cell divisions without replenishment of the PTM, would in fact provide daughter, granddaughter and great-granddaughter cells with their distinct level of the given PTM (Fig. 6E), which would indicate how many cell divisions they have gone through, and might facilitate synchronous replication. After three to four rounds of replication and cell divisions the PTM level would be depleted (Fig. 6E), and fall below a needed threshold for co-ordinated behaviour. This would coincide with cells reaching the transition zone. Such a molecular mechanism, where dilution of a chromatin mark function as a counter to monitor cell divisions, was recently demonstrated to function over a few cell divisions in the precise timing of termination of the Arabidopsis floral meristems (Sun et al., 2014; Zhang, 2014).

CONCLUSIONS

It remains to be investigated whether ASHR3-dependent H3K36 methylation can function as a cell-generation mark or cell cycle counter in the root meristem (Fig. 6E). It is however evident that *ASHR3* contributes to higher-order synchronization of replication and cell division in the MZ. Two neighbouring cells that grow at the same rate are likely to reach a size threshold at the same time, and therefore replicate at the same time. But in *ashr3-1* RAM cell layers co-replicating duplets were overrepresented, and the frequencies of categories and the distribution of co-replicating cells deviated very strongly from the Wt pattern (Table II). Additionally, neighbouring cells expressing CYCB1;1-GUS or undergoing cytokinesis were

underrepresented in the mutant compared to Wt. Together this resulted in shorter mature MZs and reduction in total root length, indicating that such co-ordination contributes to normal root growth.

Reduced meristematic activity found in certain mutants (e.g. *wox5* or *ccs52a2*) or overexpressor lines (e.g. *CDC27a*, *CLE40*), as a result of exogenous treatment with jasmonic acid, or by down-regulation of RBR1; has been associated with cell divisions in the QC, loss of stem cell activity followed by differentiation of columella initials to starch filled CRC, and consumption of the SCN (Haecker et al., 2004; Wildwater et al., 2005; Rojas et al., 2009; Stahl et al., 2009; Vanstraelen et al., 2009; Chen et al., 2011; Cruz-Ramirez et al., 2013). Normally Wt QC cells divide 2-3.6 fold less frequently than stem cells, and to have a quarter to a tenfold lower division rate than the transit amplifying cells of the MZ (Dolan et al., 1993; Fujie et al., 1993; Cruz-Ramirez et al., 2013). Intriguingly, the increased replication frequency of QC cells in the *ashr3-1* mutant was not associated with differentiation of CRC initials, supporting that consumption of the SCN is not strictly a necessary consequence of release of QC quiescence (Cruz-Ramirez et al., 2013). The stem cell niche has been described as two meristems in one, the proximal meristem and the root cap meristem (Bennett and Scheres, 2010). Interestingly, the additional QC cells in the *ashr3-1* mutant are found at the flanks of the QC near the initials of outer cell files of the proximal meristem. QC cells may be in fact be considered a stem cell reservoir that can be activated upon damage of initial cells, and be induced to divide more frequently under stressful conditions (Heyman et al., 2013). This may indicate that loss of synchronised replication, reduced cell division rate of *ashr3-1* is perceived as stress, leading to a release of the mitotic QC block, as a secondary effect of the mutation.

MATERIALS AND METHODS

Plant Material and Constructs

Wild-type (Col-0) and transgenic Arabidopsis plants were cultivated as described in (Kumpf et al., 2013). The *pASHR3:GUS* construct containing 2054 bp of promoter (Thorstensen et al., 2006), was used to generate more transgenic lines. Consistently these lines showed tapetum and lateral root expression as previously shown (Thorstensen et al., 2006), and expression in the SCN as described here. *ashr3-1* mutant plants are homozygous for the T-DNA insertion in the SAIL_804_D06 line (Fig. S1A). Wild type plants segregating from this line were used as control. The mutant phenotypes were complemented with a genomic fragment encompassing the promoter (cf. above) and the transcribed region of *ASHR3* cloned in the T-DNA vector pGSC1704 (Fig. S1).

The CycB1;1-GUS reporter (line FA4C) has 1.2 kb promoter and coding sequences of the first 116 amino acids (including the mitotic destruction box) of *CycB1;*1 in translational fusion with the *uid* gene encoding β-glucuronidase (Colón-Carmona et al., 1999). The *e2fa-2* (GABI_348E09) and *e2fb-1* (SALK_103138) mutants were described previously (Berckmans et al., 2011; Berckmans et al., 2011), the *e2fa-2 e2fb-1* double mutant was generated by crossing (Heyman et al., 2011). The *pE2Fa:E2Fa-GFP* construct was described previously (Magyar et al., 2012).

Quantitative reverse transcriptase PCR (qRT-PCR) to determine real-time transcript levels was performed essentially as in (Grini et al., 2009). Total RNA was extracted from one-week-old seedlings using the RNeasy Kit (Qiagen). After DNase treatment by thy RQ1 RNase-Free DNase (Promega), cDNA was synthesized using Supersscript III (Life Technologies) or the iScript cDNA Synthesis Kit (Bio-Rad). Relative expression levels were determined with the LightCycler 480 Real-Time SYBR green PCR System (Roche). For normalization, the genes At1G04850 and At5g18800, or were used, namely ACT

(At3G18780), CAK2 (At3G50000) and PAC1 (At3G22110) were used. *UVI4* was used as a positive control (Heyman et al., 2011)

Electrophoretic Mobility Shift Assay (EMSA)

The E2Fa and DPa coding sequences, cloned into the pDEST17 and pGBKT7 expression vectors, respectively, were used as templates for protein expression using the TnT® Quick Coupled Transcription/Translation System (Promega). A mock reaction with an empty pDEST17 vector was used as control. 250 ng of the Wt oligo 5'-aggacaaaTCTCCCGCCttaaattc-3' with the putative E2Fa binding site was labelled at the 5' end using 32P-ATP and T4 polynuclotide kinase (NEB). For assessment of binding 200 ng DPa and 300 ng E2Fa, 2.5 ng labelled probe, with or without 250 ng unlabeled Wt or mutant (5'-aggacaaaTCTCCATCCttaaattc-3') competitor, was incubated in 20 mM Tris pH 7.5, 12% glycerol, 50 mM KCl, 1 mM MgCl2, 1 mM EDTA and 0.2 mM DTT 5 min. at room temperature and 30 min. at 4 ^{o}C. The reactions were run on a 5% polyacylamid gel.

Flow cytometric analysis

Flow cytometric analysis was performed with Arabidopsis suspension cell synchronized with aphidicolin according to (Porceddu et al., 2001).

Cell File Analyses

Roots were stained with 10μM propidium iodine and images were taken with a confocal microscope (Zeiss LSM 710 and 780) and analysed with the software Zen 2009 and ImageJ.

A new plug-in for ImageJ facilitating cell file analysis has been provided by Centre for Plant Integrative Biology (CPIB), Nottingham, UK.

GUS, EdU and Lugol Staining

GUS assays were performed as described previously (Beeckman and Engler, 1994; Malamy and Benfey, 1997). GUS stained seedlings were viewed using differential interference contrast optics as described previously (Beeckman and Engler, 1994). EdU staining of replicating DNA was performed according to the manual of Click-iT® EdU Alexa Fluor® 647 Flow Cytometry Assay Kit (Invitrogen Catalog Number A10202). Lugol solution was applied for 45 sec to root tips which were inspected immediately for staining of amyloplasts using Nomarski optics with DIC.

***In situ* Immuno Localisation**

3 day old Arabidopsis seedlings were immune stained using anti KNOLLE primary antibody (1:200 dilution) and Oregon Green coupled anti rabbit secondary antibody (Invitrogen Cat No O6381-1:200 dilution) as described previously (Péret et al., 2012). Counter staining was done using Propidium Iodide (red). The images were taken using Leica SP2 Confocal microscope.

Chromatin Immuno Precipitation (ChIP)

ChIP to investigate binding of E2Fa transcription factors to the *ASHR3* promoter was performed with an anti-E2Fa antibody using 8-d-old plants according to the protocol of (Berckmans et al., 2011), with minor adaptations. Preclearing of the extracted nucleosomes was performed using 40µl of Dynabeads Progein G (Novex). After de-cross-linking, DNA was extracted using phenol/chloroform/isoamyl alcohol and purified using the MinElute PCR Purification Kit (Qiagen). As a negative control, immunoprecipitation was performed without

any antibody. qPCR experiments were performed on equal concentrations of total input, no antibody ChIP, and E2Fa ChIP DNA, as measured with the Quant-iT dsDNA High Sensitivity Kit (Invitrogen). Primers used for PCR amplification were designed to amplify the *ASHR3* upstream promoter region containing the consensus E2F *cis*-regulatory element, using Primer-BLAST (http://www.ncbi.nlm.nih.gov/tools/primer-blast/). *UVI4* and *ACTIN* were used a positive and negative control, respectively (Heyman et al., 2011). Normalization of enrichment relative to total input DNA was calculated as $100*2^{(Ct(input)-Ct(purified))}$.

ChIP for detection of chromatin marks was performed as described in (Veiseth et al., 2011), using one week old seedlings or inflorescences and the antibodies anti-H3K36me2 (#07-369, Upstate) and anti-H3K36me1 (ab9048, Abcam). A number of the genes tested, *AOS* (At5g42650), *AOC2* (At3g25780), *JAZ1* (At1g19180), *WRKY40* (At1g80840), have previously been shown to be regulated by ASHR3 in inflorescences using the line SALK_128444 (sdg4) (Cartagena et al., 2008). In addition we have used the constitutively expressed *ACTIN2* (At5g09810) and *TUBULIN8* (At3g26650), as well as the transcriptionally silent transposable elements *Ta3, TSI and CACTA* (Jacob et al., 2009). ChIP data were normalized against input. Primers can be found in Table SI.

Acknowledgements

Thanks go to Roy Falleth, Solveig H. Engebretsen and Noemi Skornski for technical assistance and to Viola Nähse-Kumpf for valuable suggestions regarding cell cycle investigations. We also thank Peter Doerner for the *CycB1;1-GUS* line FA4C, Gerd Jûrgens for the KNOLLE antibody, and Inderjit S. Mercy for making the complementation construct in the vector pGSC1704, which was kindly provided by Plant Genetic Systems. We acknowledge Michael Wilson, Andy French and Darren Wells at CPIB for providing the plug-in for ImageJ to measure cell sizes. We appreciate the use of the Zeiss 710 confocal microscope with Software ZEN2009 at the Confocal Microscopy Core Facility at The

Norwegian Radium Hospital, Oslo as well as the use of the Zeiss780 confocal microscope at the Bio Imaging Core at VIB, Gent, Belgium.,

Competing interest statement

The authors declare no competing financial interests

Author contributions

R.K. and T.T. designed and performed experiments and analysed data. M.A.R., J.H, H.Z.N., T.L., U.H., S.V.V., G.E. performed experiments. R.S. performed experiments and analysed data. M.J.B. and L.D.V. provided funding, analysed data and assisted in critical revising of the manuscript. R.B.A. designed the project, provided funding, designed and analysed experiments and wrote the manuscript.

Supplementary material

Figure S1. The *ashr3-1* mutant line.

Figure S2. The pattern of co-replicating cells are distorted in the *ashr3-1* mutant

Figure S3. E2Fa is expressed in the stem cell niche.

Figure S4. Expression levels of genes investigated by ChIP in roots.

Table S1. Primers.

REFERENCES

Baumbusch LO,Thorstensen T,Krauss V,Fischer A,Naumann K,Assalkhou R,Schulz I,Reuter G,Aalen RB (2001) The Arabidopsis thaliana genome contains at least 29 active genes encoding SET domain proteins that can be assigned to four evolutionarily conserved classes. Nucl Acids Res **29:** 4319-4333

Beemster GTS,Baskin TI (1998) Analysis of cell division and elongation underlying the developmental acceleration of root growth in *Arabidopsis thaliana*. Plant Physiol **116:** 1515-1526

Bennett T,Scheres B (2010) Root development--two Meristems for the price of one? *In* CPT Marja, ed, Current Topics in Developmental Biology, Vol Volume 91. Academic Press, pp 67-102

Berckmans B,De Veylder L (2009) Transcriptional control of the cell cycle. Curr Opin Plant Biol **12:** 599-605

Berckmans B,Lammens T,Van Den Daele H,Magyar Z,Bogre L,De Veylder L (2011) Light-dependent regulation of DEL1 is determined by the antagonistic action of E2Fb and E2Fc. Plant Physiol **157:** 1440-1451

Berckmans B,Vassileva V,Schmid SPC,Maes S,Parizot B,Naramoto S,Magyar Z,Kamei CLA,Koncz C,Bögre L,Persiau G,De Jaeger G,Friml J,Simon R,Beeckman T,De Veylder L (2011) Auxin-dependent cell cycle reactivation through transcriptional regulation of Arabidopsis E2Fa by lateral organ boundary proteins. Plant Cell **23:** 3671-3683

Cartagena JA,Matsunaga S,Seki M,Kurihara D,Yokoyama M,Shinozaki K,Fujimoto S,Azumi Y,Uchiyama S,Fukui K (2008) The Arabidopsis SDG4 contributes to the regulation of pollen tube growth by methylation of histone H3 lysines 4 and 36 in mature pollen. Develop Biol **315:** 355-368

Chen Q,Sun J,Zhai Q,Zhou W,Qi L,Xu L,Wang B,Chen R,Jiang H,Qi J,Li X,Palme K,Li C (2011) The basic helix-loop-helix transcription factor MYC2 directly represses *PLETHORA* expression during jasmonate-mediated modulation of the root stem cell niche in Arabidopsis. Plant Cell **23:** 3335-3352

Colón-Carmona A, You R, Haimovitch-Gal T, Doerner P (1999) Spatio-temporal analysis of mitotic activity with a labile cyclin–GUS fusion protein. Plant J **20:** 503-508

Costas C,de la Paz Sanchez M,Stroud H,Yu Y,Oliveros JC,Feng S,Benguria A,López-Vidriero I,Zhang X,Solano R,Jacobsen SE,Gutierrez C (2011) Genome-wide mapping of *Arabidopsis thaliana* origins of DNA replication and their associated epigenetic marks. Nat Struct Mol Biol **18:** 395-400

Costas C,Desvoyes B,Gutierrez C (2011) A chromatin perspective of plant cell cycle progression. Biochim Biophys Acta - Gene Reg Mechan **1809:** 379-387

Cruz-Ramirez A,Diaz-Trivino S,Wachsman G,Du Y,Arteaga-Vazquez M,Zhang H, Benjamins R,Blilou I,Neef AB,Chandler V,Scheres B (2013) A SCARECROW-RETINOBLASTOMA protein network controls protective quiescence in the Arabidopsis root stem cell organizer. PLoS Biol **11:** 1544-9173

De Veylder L,Beeckman T,Beemster GTS,de Almeida Engler J,Ormenese S,Maes S, Naudts M,Van Der Schueren E,Jacqmard A,Engler G,Inze D (2002) Control of proliferation, endoreduplication and differentiation by the Arabidopsis E2Fa-DPa transcription factor. EMBO J **21:** 1360-1368

De Veylder L, Larkin JC, Schnittger A (2011) Molecular control and function of endoreplication in development and physiology. Trends Plant Sci **16:** 624-634

del Pozo JC,Diaz-Trivino S,Cisneros N,Gutierrez C (2006) The balance between cell division and endoreplication depends on E2FC-DPB, transcription factors regulated by the Ubiquitin-SCFSKP2A pathway in Arabidopsis. Plant Cell **18:** 2224-2235

Dorn ES,Cook JG (2011) Nucleosomes in the neighborhood: new roles for chromatin modifications in replication origin control. Epigenetics **6:** 552-559.

Haecker A,GroÃŸ-Hardt R,Geiges B,Sarkar A,Breuninger H,Herrmann M,Laux T (2004) Expression dynamics of *WOX* genes mark cell fate decisions during early embryonic patterning in *Arabidopsis thaliana*. Develop **131:** 657-668

Hake SB,Allis CD (2006) Histone H3 variants and their potential role in indexing mammalian genomes: The "H3 barcode hypothesis". Proc Natl Acad Sci **103:** 6428-6435

Hayashi K,Hasegawa J,Matsunaga S (2013) The boundary of the meristematic and elongation zones in roots: endoreduplication precedes rapid cell expansion. Sci Rep **3:** 2723

Heyman J,Cools T,Vandenbussche F,Heyndrickx KS,Van Leene J,Vercauteren I, Vanderauwera S,Vandepoele K,De Jaeger G,Van Der Straeten D,De Veylder L (2013) ERF115 controls root quiescent center cell division and stem cell replenishment. Science **342:** 860-863

Heyman J,De Veylder L (2012) The anaphase-promoting complex/cyclosome in control of plant development. Mole Plant **5:** 1182-1194

Heyman J,Van den Daele H,De Wit K,Boudolf V,Berckmans B,Verkest A,Alvim Kamei CL,De Jaeger G,Koncz C,De Veylder L (2011) Arabidopsis *ULTRAVIOLET-B-INSENSITIVE4* maintains cell division activity by temporal inhibition of the anaphase-promoting complex/cyclosome. Plant Cell **23:** 4394-4410

Jacob Y,Feng S,LeBlanc CA,Bernatavichute YV,Stroud H,Cokus S,Johnson LM, Pellegrini M,Jacobsen SE,Michaels SD (2009) ATXR5 and ATXR6 are H3K27 monomethyltransferases required for chromatin structure and gene silencing. Nat Struct Mol Biol **16:** 763-768

Jacob Y,Stroud H,LeBlanc C,Feng S,Zhuo L,Caro E,Hassel C,Gutierrez C,Michaels SD,Jacobsen SE (2010) Regulation of heterochromatic DNA replication by histone H3 lysine 27 methyltransferases. Nature **466:** 987-991

Jiang K,Feldman LJ (2005) Regulation of root apical meristem development. Annu Rev Cell Dev Biol **21:** 485-509

Kim HS,Rhee DK,Jang YK (2008) Methylations of histone H3 lysine 9 and lysine 36 are functionally linked to DNA replication checkpoint control in fission yeast. Biochem Biophys Res Commun **368:** 419-425

Kouzarides T (2007) Chromatin modifications and their function. Cell **128:** 693-705

Lauber MH, Waizenegger I, Steinmann T, Schwarz H, Mayer U, Hwang I, Lukowitz W, Jürgens G (1997) The Arabidopsis KNOLLE protein is a cytokinesis-specific syntaxin. J Cell Biol **139:** 1485-1493

Liu CY,Lu FL,Cui X,Cao XF (2010) Histone methylation in higher plants. Annu Rev Plant Biol, **61:** 395-420

Magyar Z,DeVeylder L,Atanassova A,Bakó L,Inzé D,Bögre L (2005) The role of the Arabidopsis E2Fb transcription factor in regulating auxin-dependent cell division. The Plant Cell **17:** 2527-2541

Magyar Z, Horvath B, Khan S, Mohammed B, Henriques R, De Veylder L, Bako L, Scheres B, Bogre L (2012) Arabidopsis E2FA stimulates proliferation and endocycle separately through RBR-bound and RBR-free complexes. EMBO J **31:** 1480-1493

Menges M,Hennig L,Gruissem W,Murray JAH (2003) Genome-wide gene expression in an Arabidopsis cell suspension. Plant Mol Biol **53:** 423-442

Moubayidin L,Perilli S,Dello Ioio R,Di Mambro R,Costantino P,Sabatini S (2010) The rate of cell differentiation controls the Arabidopsis root meristem growth phase. Curr Biol **20:** 1138-1143

Naouar N,Vandepoele K,Lammens T,Casneuf T,Zeller G,Van Hummelen P,Weigel D,Rätsch G,Inzé D,Kuiper M,De Veylder L,Vuylsteke M (2009) Quantitative RNA expression analysis with Affymetrix Tiling 1.0R arrays identifies new E2F target genes. Plant J **57:** 184-194

Nawy T,Lee J-Y,Colinas J,Wang JY,Thongrod SC,Malamy JE,Birnbaum K,Benfey PN (2005) Transcriptional profile of the Arabidopsis root quiescent center. Plant Cell **17:** 1908-1925

Oh S,Park S,van Nocker S (2008) Genic and global functions for Paf1C in chromatin modification and gene expression in Arabidopsis. PLoS Genetics **4:** e1000077.

Péret B, Swarup K, Ferguson A, Seth M, Yang Y, Dhondt S, James N, Casimiro I, Perry P, Syed A, Yang H, Reemmer J, Venison E, Howells C, Perez-Amador MA, Yun J, Alonso J, Beemster GTS, Laplaze L, Murphy A, Bennett MJ, Nielsen E, Swarup R (2012) *AUX/LAX* genes encode a family of auxin influx transporters that perform distinct functions during Arabidopsis development. Plant Cell **24:** 2874-2885

Perilli S,Di Mambro R,Sabatini S (2012) Growth and development of the root apical meristem. Curr Opin Plant Biol **15:** 17-23

Perilli S,Sabatini S (2010) Analysis of root meristem size development. Methods Mol Biol **655:** 177-187

Pryde F,Jain D,Kerr A,Curley R,Mariotti FR,Vogelauer M (2009) H3 K36 methylation helps determine the timing of Cdc45 association with replication origins. PLoS ONE **4:** e5882

Raynaud C,Sozzani R,Glab N,Domenichini S,Perennes C,Cella R,Kondorosi E, Bergounioux C (2006) Two cell-cycle regulated SET-domain proteins interact with proliferating cell nuclear antigen (PCNA) in Arabidopsis. Plant J **47:** 395-407

Rojas C,Eloy N,de Freitas Lima M,Rodrigues R,Franco L,Himanen K,Beemster G, Hemerly A,Ferreira P (2009) Overexpression of the *Arabidopsis* anaphase

promoting complex subunit *CDC27* increases growth rate and organ size. Plant Mol Biol **71:** 307-318

Stahl Y,Wink RH,Ingram GC,Simon R (2009) A signaling module controlling the stem cell niche in Arabidopsis root meristems. Curr Biol **19:** 909-914

Sun B, Looi L-S, Guo S, He Z, Gan E-S, Huang J, Xu Y, Wee W-Y, Ito T (2014) Timing mechanism dependent on cell division is invoked by Polycomb eviction in plant stem cells. Science **343**

Thorstensen T,Grini PE,Aalen RB (2011) SET domain proteins in plant development. Biochim Biophys Acta - Gene Reg Mech **1809:** 407-420

Thorstensen T,Grini PE,Mercy IS,Alm V,Erdahl S,Aasland R,Aalen RB (2008) The Arabidopsis SET domain protein ASHR3 is involved in stamen development and interacts with the bHLH transcription factor ABORTED MICROSPORES (AMS). Plant Mol Biol **66:** 47-59

Ubeda-Tomas S,Federici F,Casimiro I,Beemster GTS,Bhalerao R,Swarup R,Doerner P,Haseloff J,Bennett MJ (2009) Gibberellin signaling in the endodermis controls Arabidopsis root meristem size. Current Biology **19:** 1194-1199

Vandepoele K,Vlieghe K,Florquin K,Hennig L,Beemster GTS,Gruissem W,Van de Peer Y,Inze D,De Veylder L (2005) Genome-wide identification of potential plant E2F target genes. Plant Physiol **139:** 316-328

Vanstraelen M,Baloban M,Da Ines O,Cultrone A,Lammens T,Boudolf Vr,Brown SC,De Veylder L,Mergaert P,Kondorosi E (2009) APC/CCCS52A complexes control meristem maintenance in the Arabidopsis root. Proc Natl Acad Sci **106:** 11806-11811

Veiseth SV, Rahman MA, Yap KL, Fischer A, Egge-Jacobsen W, Reuter G, Zhou MM, Aalen RB, Thorstensen T (2011) The SUVR4 histone lysine methyltransferase binds ubiquitin and converts H3K9me1 to H3K9me3 on transposon chromatin in Arabidopsis. PLoS Genet **7:** e1001325

Verkest A,Abeel T,Heyndrickx K,Van Leene J,Lanz C,Van De Slijke E,De Winne N, Eeckhout D,Persiau G,Van Breusegem F,Inze D,Vandepoele K,De Jaeger G (2014) A generic tool for transcription factor target gene discovery in Arabidopsis cell suspension cultures based on tandem chromatin affinity purification. Plant Physiol PMID: 24453163

Weinberg RA, (1995) The Retinoblastoma Protein and cell cycle control. Cell Res **81:** 323-330

Wildwater M,Campilho A,Perez-Perez JM,Heidstra R,Blilou I,Korthout H,Chatterjee J,Mariconti L,Gruissem W,Scheres B (2005) The *RETINOBLASTOMA-RELATED* gene regulates stem cell maintenance in Arabidopsis roots. Cell **123:** 1337-1349

Zhang X (2014) Delayed gratification—waiting to terminate stem cell identity. Science **343:** 498-499

Figure legends

Figure 1. *ASHR3* is expressed in the root stem cell niche (SCN) and influences meristem cell size and root length.

A, Expression of *pASHR3:GUS* in the SCN, with close-up (lower panel). Endo – endodermis; Cor – cortex; Epi – epidermis; LRC – lateral root cap; CRC – columella root cap; QC – quiescent centre. B, Length of primary root of Wt, *ashr3-1*, and the mutant complemented with the Wt gene (*ashr3-1 ASHR3)* at 3, 6 and 10 days after germination (DAG). N = 17, 24, and 26, respectively. Standard deviations are indicated. Statistical differences are marked with *: The *ashr3-1 ASHR3* line was statistically equal to Wt (Student's *t*-test P = 0.49), and, like the Wt, significantly longer than the mutant (P = 0.037 and P = 0.015, respectively). C, Cortical meristematic cell length. The average size of cortical cells, number 1-28 after the initial, was determined from measurements of 9 *ashr3-1* and 10 Wt cortical files of 6 DAG primary roots. The graph shows the mean of four consecutive cells with standard deviations. (* P < 0.05; ** <0.01). D, Propidium iodide (PI) stained root meristems of Wt and *ashr3-1* seedlings at 6 DAG. The QC and the transition zone (TZ) are indicated. E, PI stained Wt and *ashr3-1* root tips and SCN (lower panel). Arrows point at aberrant cell patterns.

Figure 2. DNA replication and cell division patterns are distorted in *ashr3-1* root meristems.

A, Distribution of replicating cells along Wt and *ashr3-1* cortical meristematic cell files of 10 days old roots as percentage of total number of cells, starting from the stem cell and delimited to 40 cells. Wt - two sets with n = 8 cell files, from 9 roots; *ashr3-1* – two sets with n = 9 files, from 10 roots; total number of replicating cells n_{Wt} = 206, $n_{ashr3\text{-}1}$ = 161. Standard deviations are indicated. B, Representative confocal images of primary root meristems of Wt and *ashr3-1* seedlings as indicated, incubated for 1 hour with EdU. Examples of neighboring replicating cells, duplets (2), quartets (4) and octets (8), are indicated. Cells without replicating neighbours (singlets) were dominating in the boxed areas. Meta- and anaphases are

encircled. C, Frequencies of singlets and categories of co-replicating cortical cells in Wt and *ashr3-1* cell files. D, and E, Distribution of singlets and neighbouring, co-replicating cells (duplets, quartets and octets) along Wt and *ashr3-1* cortical cell files, as indicated, as percentage of the total number of replicating cells. For simplicity, triplets and sextets have been omitted. Compiled data for 16 Wt cortical cell files from 9 roots, and 18 *ashr3-1* cortical cell files from 10 roots. F, Region with CYCB1;1-GUS expression in Wt and *ashr3-1* root tips. G, MZ of Wt and *ashr3-1* roots expressing CYCB1;1-GUS. Arrowheads indicate the end of the MZ. H, and I, *in situ* immuno localization of KNOLLE (green) in 3 DAG MZ. Counter staining was done using propidium iodide (red). Single focus plane (H) and maximum projection (I) images were generated using Leica Confocal software. Bars 20µM.

Figure 3. *ASHR3* maintains QC quiescence.

A, B, Representative Wt and *ashr3-1* images, respectively, of SCN and surrounding tissue. Nuclei in the QC and stem cell layer of the columella root cap (CRC layer D1) are indicated by black stars. C, Expression of the *pWOX5:GUS* and *QC46:GUS* QC marker lines in Wt and *ashr3-1* as indicated. Peri – pericycle; Endo – endodermis; Cor – cortex; Epi – epidermis; LRC – lateral root cap. D, E, Representative images of Wt and *ashr3-1* SCN with DAPI stained nuclei (blue) after 1 hours treatment with EdU (depicted in green). Nuclei in the QC and CRC stem cell layer are indicated by red and white stars, respectively. F, G, Representative images of seven days old Wt and *ashr3-1* root tips, respectively, after Lugol staining of the starch granules in differentiated CRC cells. Nuclei in the QC and CRC stem cell layer (D1) are indicated by red and white stars, respectively.

Figure 4. *ASHR3* expression is cell-cycle dependently regulated by E2Fa-DPa.

A, Quantitative RT-PCR (qRT-PCR) monitoring *ASHR3* transcript levels during the cell cycle in Arabidopsis cell suspensions synchronized using aphidicolin. Transcript levels were

determined every second hour after aphidicolin removal. In parallel the C value (haploid DNA content) of the cells was determined by flow cytometry. B, Relative expression level of *ASHR3* determined by qRT-PCR in a line overexpressing E2Fa-DPa (De Veylder et al., 2002) and in one-week old *e2fa-2* and *e2fb-1* single and *e2fa-2 e2fb-1* double mutant seedlings compared to Wt level, which was set to one. *UVI4* was included as a positive control (Heyman et al., 2011). Data represent mean ± SE (*n*=3). C, Electrophoretic mobility shift assay (EMSA) using *in vitro* expressed E2Fa-DPa, a ^{32}P-labelled oligo-nucleotide corresponding to an *ASHR3* promoter fragment with a putative E2Fa-DPa binding site, and unlabelled competitor sequence with or without a two nucleotide mutation. + indicates the presence and – the absence of a given ingredient in the reaction prior to gel electrophoresis. Stars indicate unspecific binding of the probe, and the arrow the protein:DNA complex that can be competed with non-labeled Wt, but not with a mutant oligonucleotide. D, Enrichment of the promoter region encompassing the promoter fragment of *ASHR3* used in C, relative to input after ChIP from one-week old seedlings with an E2Fa antibody, and with an no-antibody control. The promoters of *ACTIN2* and *UVI4* were used as negative and positive controls, respectively.

Figure 5. *ASHR3*-dependent mono- and dimethylation of histone H3 lysine 36.

ChIP analysis of Wt and *ashr3-1* chromatin from seedlings using antibodies against A, H3K36me1 and B, H3K36me2 as indicated. DNA levels from the experiment relative to the input reactions were quantified using qRT-PCR. The bars represent the average of two to three independent biological replicates. Standard deviations are indicated.

Figure 6. Working model for synchronized DNA replication and division of progeny cells along the cell files of the outer layers of the root MZ.

A, DNA replication takes place in the whole MZ in an organized pattern. The first few cells that are direct progeny of the stem cell, replicate unco-ordinately as singlets, and give rise to four pairs of daughter cells (duplets) for which sister cells will replicate co-ordinately. They will in turn give rise to four sets of granddaughter cells (quartets), each with co-ordinated sister-cell replication, which subsequently results in four sets of co-replicating great-granddaughters. At the borders of singlets and duplets, triplets can accidently occur, and likewise sextets will arise between duplets and quartets. The arrowhead indicates the end of the MZ. B, The expression pattern of CYCB1;1-GUS suggests that mitosis only occur in singlet, duplet and quartet cells. C, Cytokinesis is also confined to singlets, duplets and quartets, here demonstrated by localisation of KN-GFP in novel cell plates during the generation of quartets from duplets. D, DNA replication without cell division results in endoreduplication in the octet region, as also suggested by Hayashi et al. (2013) from the intensity of EdU staining, cell size and size of replicating nuclei. E, ASHR3 is needed for the co-ordinated DNA replication and cell division as indicated by the absent cell walls in *ashr3-1* (*) compared to Wt (see A). Theoretically, methylation of H3K36 by ASHR3 at specific targets in nuclei in the SCN, without renewal in the MZ cells, could work as a counter of cell divisions and identifier of sister cells, as the level of the mark will be halved during each round of replication, providing each cell with a generation-specific and ASHR3-dependent H3K36me level. This hypothesis remains to be tested.

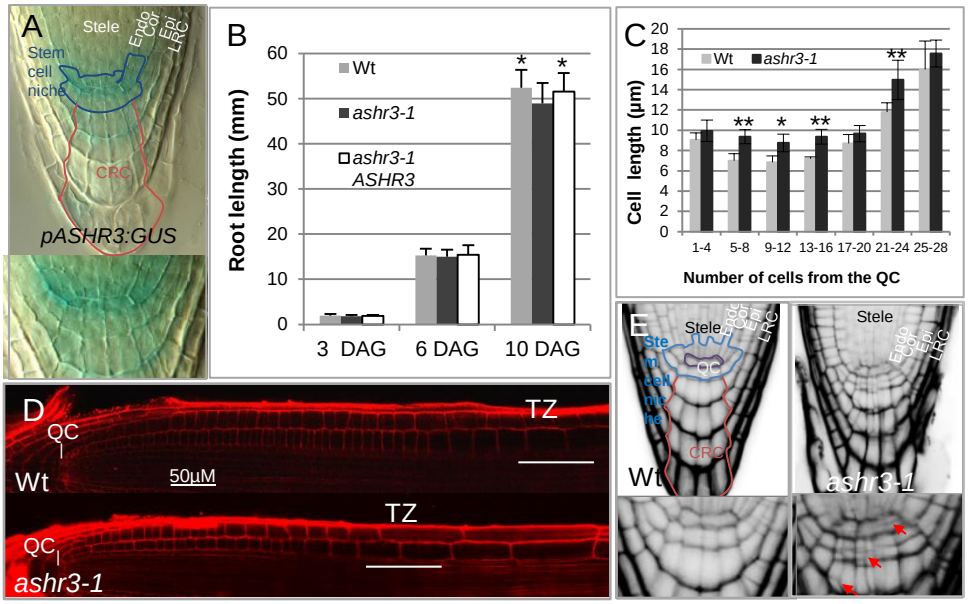

Figure 1. *ASHR3* is expressed in the root stem cell niche (SCN) and influences meristem cell size and root length.
A, Expression of *pASHR3:GUS* in the SCN, with close-up (lower panel). Endo – endodermis; Cor – cortex; Epi – epidermis; LRC – lateral root cap; CRC – columella root cap; QC – quiescent centre. B, Length of primary root of Wt, *ashr3-1,* and the mutant complemented with the Wt gene (*ashr3-1 ASHR3)* at 3, 6 and 10 days after germination (DAG). N = 17, 24, and 26, respectively. Standard deviations are indicated. Statistical differences are marked with *: The *ashr3-1 ASHR3* line, was statistically equal to Wt (Student's *t*-test P = 0.49), and, like the Wt, significantly longer than the mutant (P = 0.037 and P = 0.015, respectively). C, Cortical meristematic cell length. The average size of cortical cells, number 1-28 after the initial, was determined from measurements of 9 *ashr3-1* and 10 Wt cortical files of 6 DAG primary roots. The graph shows the mean of four consecutive cells with standard deviations. (* P < 0.05; ** <0.01). D, Propidium iodide (PI) stained root meristems of Wt and *ashr3-1* seedlings at 6 DAG. The QC and the transition zone (TZ) are indicated. E, PI stained Wt and *ashr3-1* root tips and SCN (lower panel). Arrows point at aberrant cell patterns.

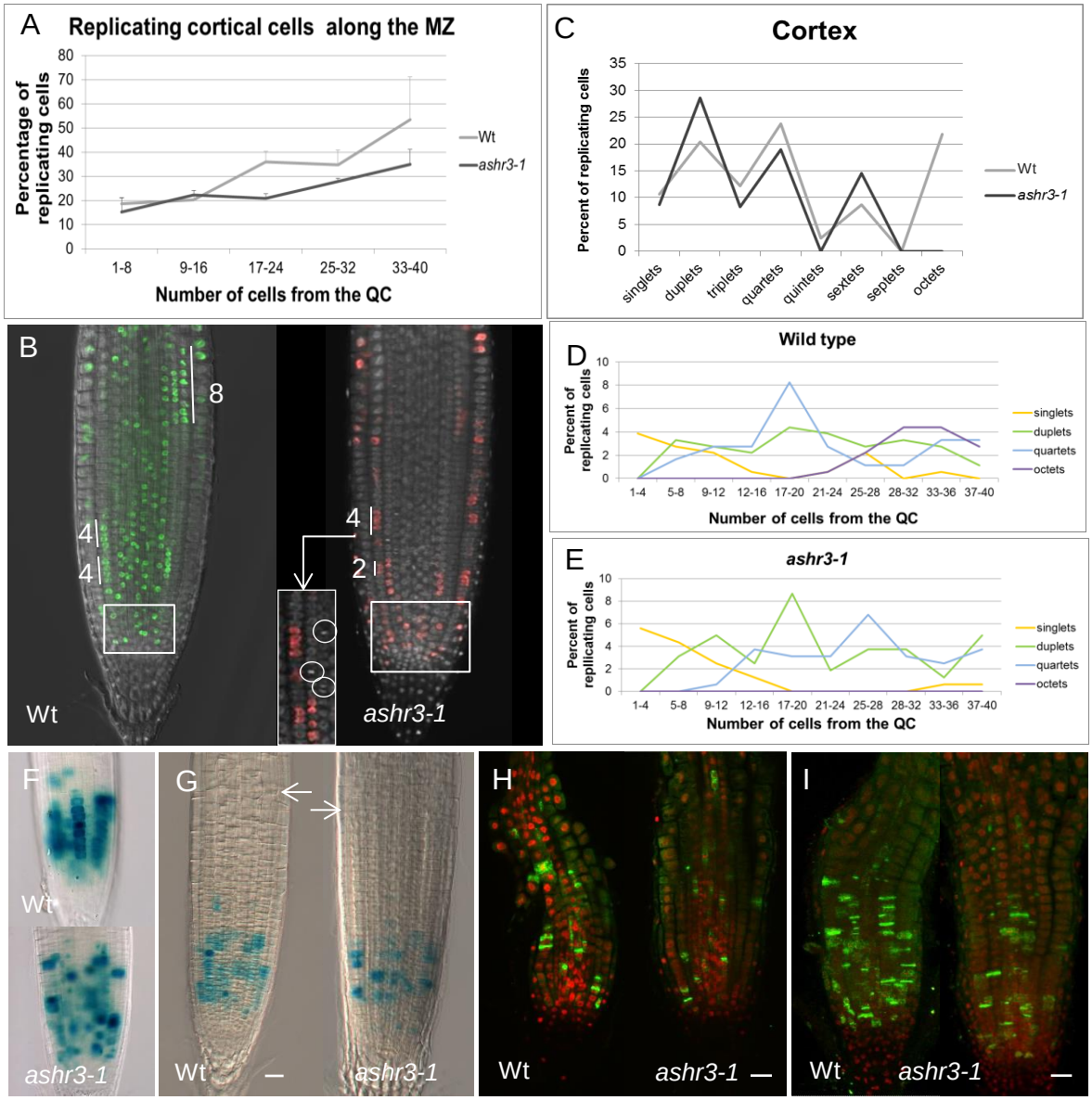

Figure 2. DNA replication and cell division patterns are distorted in *ashr3-1* root meristems.
A, Distribution of replicating cells along Wt and *ashr3-1* cortical meristematic cell files of 10 days old roots as percentage of total number of cells, starting from the stem cell and delimited to 40 cells. Wt - two sets with n = 8 cell files, from 9 roots; *ashr3-1* – two sets with n = 9 files, from 10 roots; total number of replicating cells n_{Wt} = 206, $n_{ashr3-1}$ = 161. Standard deviations are indicated. B, Representative confocal images of primary root meristems of Wt and *ashr3-1* seedlings as indicated, incubated for 1 hour with EdU. Examples of neighboring replicating cells, duplets (2), quartets (4) and octets (8), are indicated. Cells without replicating neighbours (singlets) were dominating in the boxed areas. Meta- and anaphases are encircled. C, Frequencies of singlets and categories of co-replicating cortical cells in Wt and *ashr3-1* cell files. D, and E, Distribution of singlets and neighbouring, co-replicating cells (duplets, quartets and octets) along Wt and *ashr3-1* cortical cell files, as indicated, as percentage of the total number of replicating cells. For simplicity, triplets and sextets have been omitted. Compiled data for 16 Wt cortical cell files from 9 roots, and 18 *ashr3-1* cortical cell files from 10 roots. F, Region with CYCB1;1-GUS expression in Wt and *ashr3-1* root tips. G, MZ of Wt and *ashr3-1* roots expressing CYCB1;1-GUS. Arrowheads indicate the end of the MZ. H, and I, *in situ* immuno localization of KNOLLE (green) in 3 DAG MZ. Counter staining was done using propidium iodide (red). Single focus plane (H) and maximum projection (I) images were generated using Leica Confocal software. Bars 20µM.

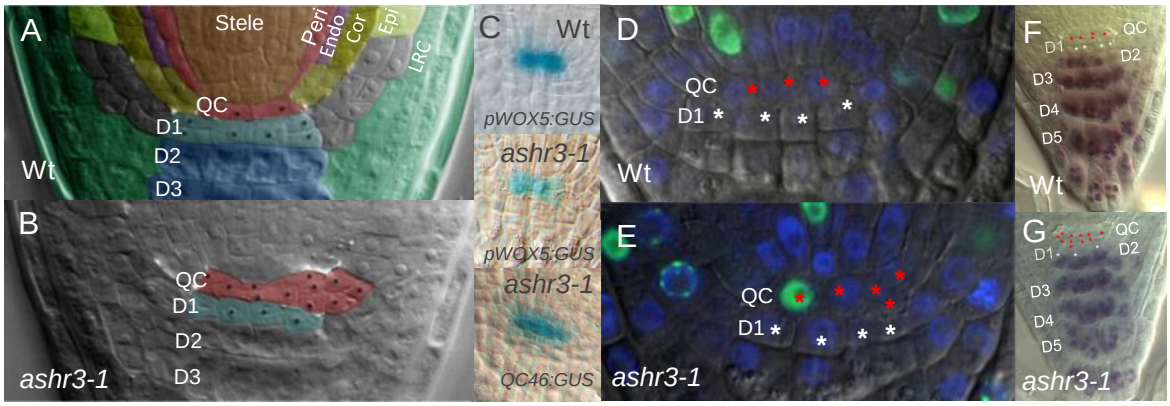

Figure 3. *ASHR3* maintains QC quiescence.
A, B, Representative Wt and *ashr3-1* images, respectively, of SCN and surrounding tissue. Nuclei in the QC and stem cell layer of the columella root cap (CRC layer D1) are indicated by black stars. C, Expression of the *pWOX5:GUS* and *QC46:GUS* QC marker lines in Wt and *ashr3-1* as indicated. Peri – pericycle; Endo – endodermis; Cor – cortex; Epi – epidermis; LRC – lateral root cap. D, E, Representative images of Wt and *ashr3-1* SCN with DAPI stained nuclei (blue) after 1 hours treatment with EdU (depicted in green). Nuclei in the QC and CRC stem cell layer are indicated by red and white stars, respectively. F, G, Representative images of seven days old Wt and *ashr3-1* root tips, respectively, after Lugol staining of the starch granules in differentiated CRC cells. Nuclei in the QC and CRC stem cell layer (D1) are indicated by red and white stars, respectively.

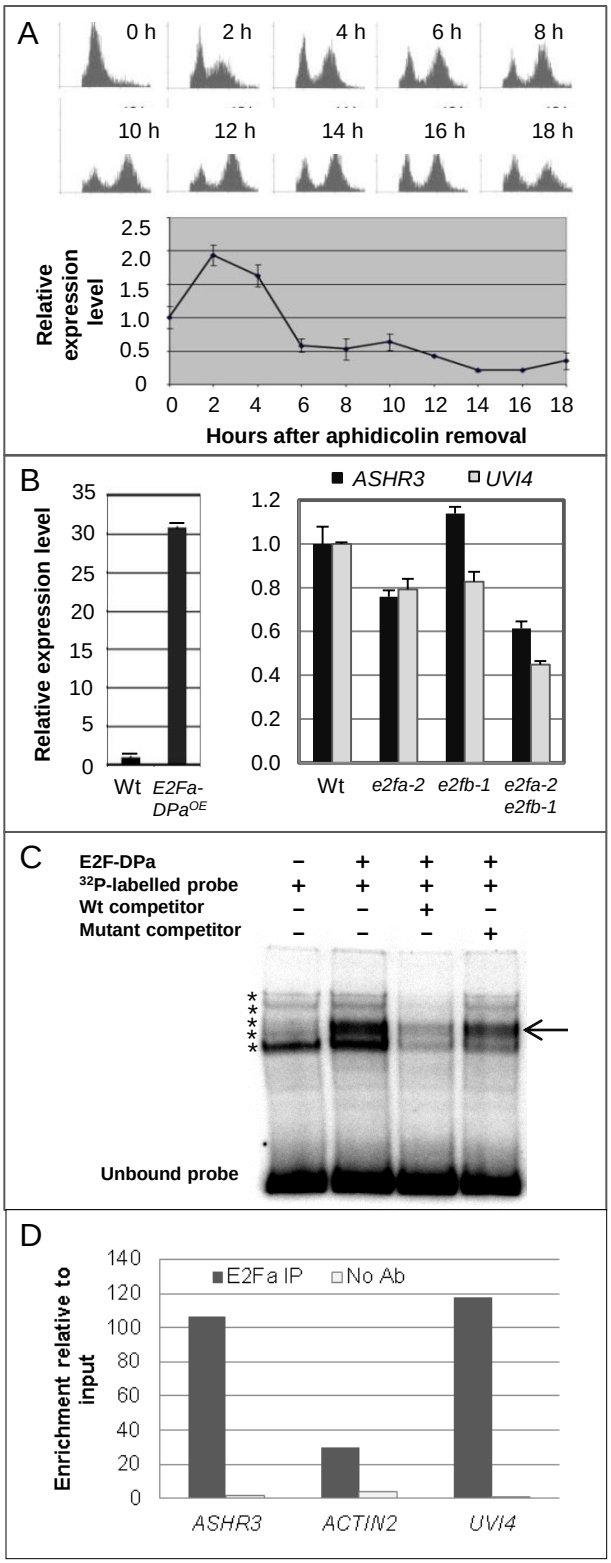

Figure 4. *ASHR3* expression is cell-cycle dependently regulated by E2Fa-DPa. A, Quantitative RT-PCR (qRT-PCR) monitoring *ASHR3* transcript levels during the cell cycle in Arabidopsis cell suspensions synchronized using aphidicolin. Transcript levels were determined every second hour after aphidicolin removal. In parallel the C value (haploid DNA content) of the cells was determined by flow cytometry. B, Relative expression level of *ASHR3* determined by qRT-PCR in a line overexpressing E2Fa-DPa (De Veylder et al., 2002) and in one-week old *e2fa-2* and *e2fb-1* single and *e2fa-2 e2fb-1* double mutant seedlings compared to Wt level, which was set to one. *UVI4* was included as a positive control (Heyman et al., 2011). Data represent mean ± SE (*n*=3). C, Electrophoretic mobility shift assay (EMSA) using *in vitro* expressed E2Fa-DPa, a ^{32}P-labelled oligo-nucleotide corresponding to an *ASHR3* promoter fragment with a putative E2Fa-DPa binding site, and unlabelled competitor sequence with or without a two nucleotide mutation. + indicates the presence and – the absence of a given ingredient in the reaction prior to gel electrophoresis. Stars indicate unspecific binding of the probe, and the arrow the protein:DNA complex that can be competed with non-labeled Wt, but not with a mutant oligonucleotide. D, Enrichment of the promoter region encompassing the promoter fragment of *ASHR3* used in C, relative to input after ChIP from one-week old seedlings with an E2Fa antibody, and with an no-antibody control. The promoters of *ACTIN2* and *UVI4* were used as negative and positive controls, respectively.

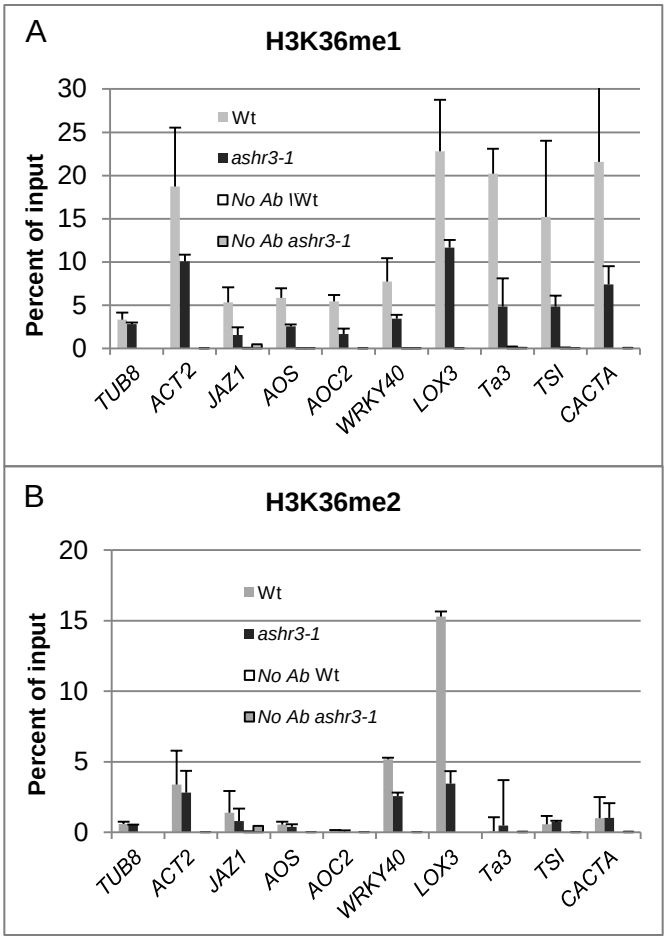

Figure 5. *ASHR3*-dependent mono- and dimethylation of histone H3 lysine 36.
ChIP analysis of Wt and *ashr3-1* chromatin from seedlings using antibodies against A, H3K36me1 and B, H3K36me2 as indicated. DNA levels from the experiment relative to the input reactions were quantified using qRT-PCR. The bars represent the average of two to three independent biological replicates. Standard deviations are indicated.

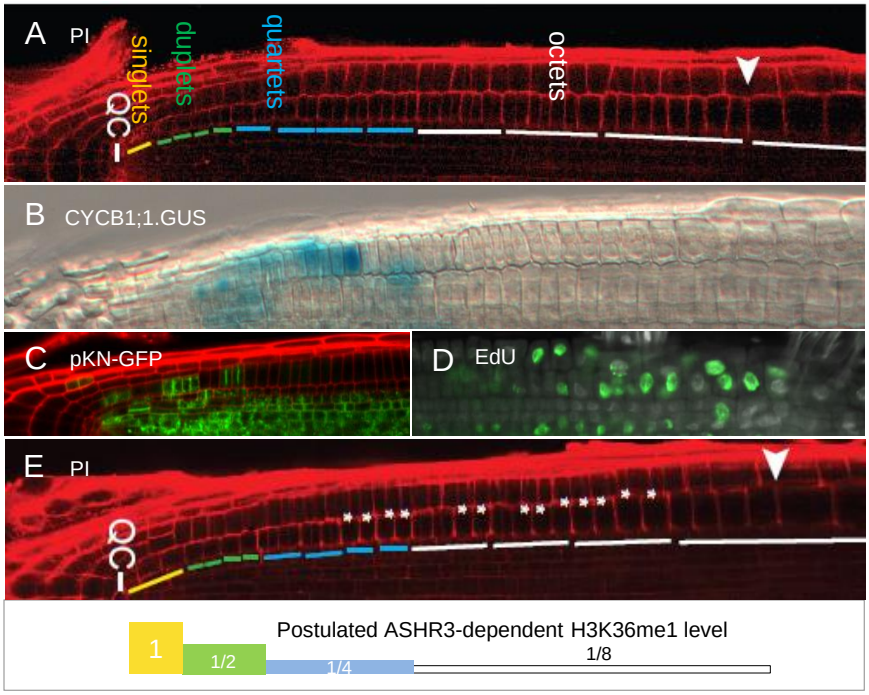

Figure 6. Working model for synchronized DNA replication and division of progeny cells along the cell files of the outer layers of the root MZ.
A, DNA replication takes place in the whole MZ in an organized pattern. The first few cells that are direct progeny of the stem cell, replicate unco-ordinately as singlets, and give rise to four pairs of daughter cells (duplets) for which sister cells will replicate co-ordinately. They will in turn give rise to four sets of granddaughter cells (quartets), each with co-ordinated sister-cell replication, which subsequently results in four sets of co-replicating great-granddaughters. At the borders of singlets and duplets, triplets can accidently occur, and likewise sextets will arise between duplets and quartets. The arrowhead indicates the end of the MZ. B, The expression pattern of CYCB1;1-GUS suggests that mitosis only occur in singlet, duplet and quartet cells. C, Cytokinesis is also confined to singlets, duplets and quartets, here demonstrated by localisation of KN-GFP in novel cell plates during the generation of quartets from duplets. D, DNA replication without cell division results in endoreduplication in the octet region, as also suggested by Hayashi et al. 2013 from the intensity of EdU staining, cell size and size of replicating nuclei. E, ASHR3 is needed for the co-ordinated DNA replication and cell division as ASHR3, as indicated by the absent cell walls in *ashr3-1* (*) compared to Wt (see A). Theoretically, methylation of H3K36 by ASHR3 at specific targets in nuclei in the SCN, without renewal in the MZ cells, could work as a counter of cell divisions and identifier of sister cells, as the level of the mark will be halved during each round of replication, providing each cell with a generation-specific and ASHR3-dependent H3K36me level. This hypothesis remains to be tested.

Table I. Expression levels in the QC relative to the surrounding tissues of *ASHR3* and selected genes with known QC expression. Data compiled from Nawy et al. 2005.

Gene	QC	Ratio*	LCR	CRC	Ground tissue	Atrichoblasts	Steele
AT5G62165 AGL42	1.0	1.7	0.6	0.4	0.7	0.6	0.9
AT4G30860 ASHR3	1.2	1.4	0.9	0.9	0.9	1.0	0.9
AT3G20840 PLETHORA	6.3	5.7	1.2	2.8	1.2	0.7	0.9
AT5G67260 CYCD3;2	4.9	2.6	1.8	1.2	2.6	2.3	2.6

* Average ratio of the QC level and the level in the other tissues

Table II. Sister-cell co-replication is dependent on *ASHR3.* Percent of replicating cells that are single or are co-replicating with neigbouring cells. The number of cells for each genotype was n_{Wt} = 348, $n_{ashr3\text{-}1}$= 129 for the cortex, n_{Wt} = 348, $n_{ashr3\text{-}1}$= 129 for the epidermis, and n_{Wt} = 265, $n_{ashr3\text{-}1}$= 232 for the endodermal cell files.

Category	Cortex		Epidermis		Endodermis	
	Wt	***ashr3-1***	**Wt**	***ashr3-1***	**Wt**	***ashr3-1***
Singlets	10.7	10.9	19.3	24.1	13.2	14.6
Duplets	20.4	36.3	28.7	46.6	24.4	37.8
Triples	12.1	10.2	7.5	7.3	7.2	11.0
Quartets	23.8	23.5	26.8	15.5	28.7	23.2
Quintets & sextets	11.2	19.1	7.1	2.6	7.2	13.4
Octets	21.8	0.0	10.6	0.0	19.3	0.0
Total	100	100	100	100	100	100
χ2 test *ashr3-1* vs Wt	-	1.4E-07	-	1.2E-05	-	1.4E-06
χ2 test vs. Wt cortex	-	1.4E-07	0.001	1.4E-16	0.29	2.7E-07

Table III. ASHR3 may be needed for efficient cell cycle progression. Number of meta- and anaphases per root (n_{Wt}=16; $n_{ashr3\text{-}1}$=10) in different tissues of the meristem. Two-three images were inspected per root.

	Stele		**Pericycle**		**Endodermis**		**Stele+Peri+Endo**		**Cortex**		**Epidermis**		**Cortex+Epidermis**		**Total**
	Meta	**Ana**	**Meta**	**Ana**	**Meta**	**Ana**	**Meta**	**Ana**	**Meta**	**Ana**	**Meta**	**Ana**	**Meta**	**Ana**	
Wt	0.3	0.0	0.1	0.0	0.2	0.0	0.6	0.0	0.2	0.0	0.3	0.0	0.4	0.0	1.0
ashr3-1	1.1	0.8	0.7	0.2	0.6	0.0	2.4	1.0	0.1	0.0	0.1	0.0	0.2	0.0	3.6